β-decay scheme of ^{140}Te to ^{140}I: Suppression of Gamow-Teller transitions between the neutron $h_{9/2}$ and proton $h_{11/2}$ partner orbitals

B. Moon,[1] C.-B. Moon,[2,*] A. Odahara,[3] R. Lozeva,[4,5] P.-A. Söderström,[6,7] F. Browne,[6,8] C. Yuan,[9] A. Yagi,[3] B. Hong,[1] H. S. Jung,[10] P. Lee,[10] C. S. Lee,[10] S. Nishimura,[6] P. Doornenbal,[6] G. Lorusso,[6] T. Sumikama,[6] H. Watanabe,[6] I. Kojouharov,[11] T. Isobe,[6] H. Baba,[6] H. Sakurai,[6] R. Daido,[3] Y. Fang,[3] H. Nishibata,[3] Z. Patel,[6,12] S. Rice,[6,12] L. Sinclair,[6,13] J. Wu,[6,14] Z. Y. Xu,[15] R. Yokoyama,[16] T. Kubo,[6] N. Inabe,[6] H. Suzuki,[6] N. Fukuda,[6] D. Kameda,[6] H. Takeda,[6] D. S. Ahn,[6] Y. Shimizu,[6] D. Murai,[17] F. L. Bello Garrote,[18] J. M. Daugas,[19] F. Didierjean,[4] E. Ideguchi,[20] T. Ishigaki,[3] S. Morimoto,[3] M. Niikura,[6,15] I. Nishizuka,[21] T. Komatsubara,[6] Y. K. Kwon,[22] and K. Tshoo[22]

[1]*Department of Physics, Korea University, Seoul 02841, Republic of Korea*
[2]*Faculty of Science, Hoseo University, Chung-Nam 31499, Republic of Korea*
[3]*Department of Physics, Osaka University, Osaka 560-0043, Japan*
[4]*IPHC, CNRS, IN2P3 and University of Strasbourg, F-67037 Strasbourg Cedex 2, France*
[5]*CSNSM, CNRS/IN2P3, University Paris-Sud, F-91405 Orsay Campus, France*
[6]*RIKEN Nishina Center, Wako, Saitama 351-0198, Japan*
[7]*Technische Universität Darmstadt, D-64289 Darmstadt, Germany*
[8]*School of Computing, Engineering and Mathematics, University of Brighton, Brighton BN2 4GJ, United Kingdom*
[9]*Sino-French Institute of Nuclear Engineering and Technology, Sun Yat-Sen University, Zhuhai 519-082, China*
[10]*Department of Physics, Chung-Ang University, Seoul 06974, Republic of Korea*
[11]*GSI Helmholtzzentrum für Schwerionenforschung GmbH, D-64291 Darmstadt, Germany*
[12]*Department of Physics, University of Surrey, Guildford GU2 7XH, United Kingdom*
[13]*Department of Physics, University of York, Heslington, York YO10 5DD, United Kingdom*
[14]*School of Physics and State key Laboratory of Nuclear Physics and Technology, Peking University, Beijing 100871, China*
[15]*Department of Physics, University of Tokyo, Tokyo 113-0033, Japan*
[16]*Center for Nuclear Study, University of Tokyo, RIKEN Campus, Wako, Saitama 351-0198, Japan*
[17]*Department of Physics, Rikkyo University, Tokyo 172-8501, Japan*
[18]*Department of Physics, University of Oslo, N-0316 Oslo, Norway*
[19]*CEA, DAM, DIF, F-91297 Arpajon Cedex, France*
[20]*RCNP, Osaka University, Osaka 567-0047, Japan*
[21]*Department of Physics, Tohoku University, Sendai, Miyagi 980-8578, Japan*
[22]*Rare Isotope Science Project, Institute for Basic Science, Daejeon 34047, Republic of Korea*

(Received 3 April 2017; revised manuscript received 23 May 2017; published 31 July 2017)

We report for the first time the β-decay scheme of ^{140}Te ($Z = 52$) to ^{140}I ($Z = 53$), with a specific focus on the Gamow-Teller strength along $N = 87$ isotones. These results were obtained in an experiment performed at the Radioactive Ion Beam Factory (RIBF), RIKEN, where the parent nuclide, ^{140}Te, was produced through the in-flight fission of a ^{238}U beam at 345 MeV per nucleon impinging on a ^{9}Be target. Based on data from the high-efficiency γ-ray spectrometer, EUROBALL-RIKEN Cluster Array (EURICA), we constructed a decay scheme of ^{140}I. The half-life of ^{140}Te has been determined to be 350(5) ms. A level at 926 keV has been assigned as a (1^+) state based on the log ft value of 4.89(6). This (1^+) state, commonly observed in odd-odd nuclei, can be interpreted in terms of the $\pi h_{11/2}\nu h_{9/2}$ configuration formed by the Gamow-Teller transition between a neutron in the $h_{9/2}$ orbital and a proton in the $h_{11/2}$ orbital. We observe a sharp contrast to this type of β-decay branching to the lower-lying 1^+ states between ^{140}I and ^{136}I, where we see a large reduction as the number of neutrons increases. This is in contrast to the prediction by large-scale shell model calculations. To investigate this type of the suppression, results of the Nilsson model calculations will be discussed. Along the isotones with $N = 87$, we discuss a characteristic feature of the Gamow-Teller distributions at 1^+ states with respect to the isospin difference.

DOI: 10.1103/PhysRevC.96.014325

I. INTRODUCTION

Nuclear physics plays an essential role in our understanding of the origin of chemical elements in the cosmos. These elements originate from atomic nuclei produced through nuclear reactions under extremely high-temperature plasma conditions in hot stars, and their explosive events: novae, x-ray bursts, and supernovae [1–3]. In astrophysical environments, the β decay of unstable nuclei plays a crucial role in controlling nucleosynthesis. The heavy neutron-rich nuclides are known to be synthesized mostly through rapid neutron capture reactions (r process) [3–5], and the final isotopic abundances are strongly dependent on the results of a complex

*cbmoon@hoseo.edu

network of nuclear reactions and β decays. The β-decay strengths are largely influenced by the so-called Gamow-Teller (G-T) interaction. The G-T transition is closely related to the spin-isospin interaction, which is of great importance to nuclei and is crucial for estimating weak transition rates in late stellar evolution. Consequently, the complexity of the role played by the G-T transition in the late stellar nucleosynthesis requires full discussions on both the nuclear structure and nuclear astrophysics. Generally, a group of states populated by G-T transitions is concentrated in the region of a G-T giant resonance at high temperatures associated with higher-lying excited states above 5 MeV in daughter nuclei [6]. In contrast, the presence of low-lying G-T transition determines abundances produced at low temperature in the decay from the r-process path. The G-T strength has been mainly constrained by the transformation between a proton and a neutron in the high-spin orbitals such as $\pi f_{7/2}-\nu f_{7/2}$, $\pi g_{9/2}-\nu g_{9/2}$, and $\pi h_{11/2}-\nu h_{11/2}$. However, in extremely neutron-rich environments—for instance, late stages of the core collapse of massive stars—it can be controlled by the interplay between a neutron in the upper orbital and a proton in the lower orbital in a spin-orbit partner: $\pi f_{7/2}-\nu f_{5/2}$, $\pi g_{9/2}-\nu g_{7/2}$, and $\pi h_{11/2}-\nu h_{9/2}$. As 1^+ states in an odd-odd nucleus are strongly related to the G-T transition within those partners, many properties of the G-T transition such as the population, energy, and strength provide direct information on its internal structure [7].

The region outside the doubly closed shell ($Z = 50$ and $N = 82$) ^{132}Sn nucleus is the subject of renewed experimental and theoretical interest in view of shell evolution. Unpredicted interesting results, especially related to the neutron dominance beyond the ^{132}Sn region, have been revealed [8–11]. In this work, we present the first level structure of the very neutron-rich nucleus ^{140}I through the β decay of ^{140}Te with $Z = 52$ and $N = 88$. We have measured the β-decay half-life and transition intensities, to obtain log ft values for G-T strengths. In this region, the only allowed β-decay transitions, G-T transitions, involve the decay of an $h_{9/2}$ neutron to an $h_{11/2}$ proton. Such a decay from an even-even nucleus gives rise to a $[\nu h_{9/2}\pi h_{11/2}]1^+$ state in the odd-odd daughter nucleus. In the following, we will discuss the emerging features of the G-T transitions of 1^+ states in the neutron-rich odd-odd nuclei, including ^{140}I, on the basis of both theoretical calculations and phenomenological systematics.

II. EXPERIMENTAL DETAILS

The experiment was carried out at the Radioactive Isotope Beam Factory (RIBF) of the RIKEN Nishina Center. The parent nuclides, ^{140}Te, were produced from the in-flight fission of ^{238}U beams at 345 MeV per nucleon impinging on a ^{9}Be target, and selected by the first stage of the BigRIPS separator [12]. Fission fragments, transported through the BigRIPS and Zero-Degree spectrometers, were unambiguously identified by the $B\rho$-ΔE-time-of-flight method [13]. These fragments were implanted into the wide-range active silicon strip stopper array for β and ion detection (WAS3ABi), which comprised five layers of 1-mm-thick double-sided silicon-strip detectors (DSSSDs) [14]. A total of 1.8×10^6 ions for ^{140}Te were sorted among the total of $\sim 10^7$ ions in the cocktail beam. The emitted γ rays, following the β decay of ^{140}Te, were detected by the EUROBALL-RIKEN cluster array (EURICA) [15].

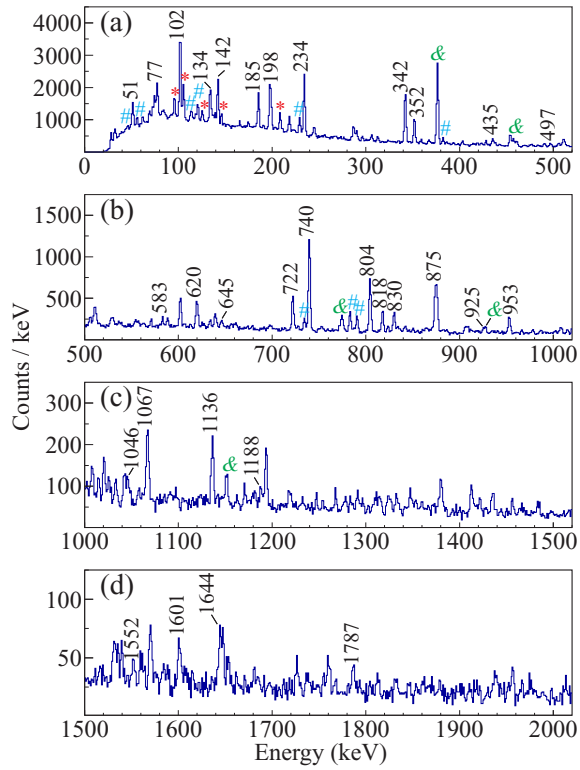

FIG. 1. Singles γ-ray spectrum following the β decay of ^{140}Te. Peaks from ^{140}I are labeled by transition energies as well as the blue sharp symbol (#). Peaks labeled with red asterisks (*) and green symbols (&) originate from the β-delayed neutron emission, ^{139}I, and the states populated in ^{140}Xe, respectively. Unmarked peaks are the room- and beam-induced backgrounds.

III. EXPERIMENTAL RESULTS

Figure 1 shows the β-delayed γ-ray spectrum of ^{140}Te. In order to sort γ-ray transitions from the internal structure of ^{140}I, only β-ray events within 500 ms after ion implantations were considered. Full energy peaks indicated by numbers or blue sharp symbols (#) are γ-ray transitions in ^{140}I. The half-life of ^{140}Te was determined to be 350(5) ms by analyzing decay curves of several transitions in ^{140}I as shown in Fig. 2. The result was obtained by using a maximum likelihood method with a fit function composed of a single-component exponential decay and a constant background. Figure 3 represents γ-γ coincidence spectra for 51, 77, 102, 134, 198, 740, 953, and 1067 keV. The 376-, 458-, and 775-keV peaks are known transitions in ^{140}Xe which is the daughter nucleus of ^{140}I. Unmarked peaks are mostly from random coincidence events or separated γ-ray energies of transitions in ^{140}Xe. For instance, in the spectrum of 198 keV, a full energy peak at 178 keV makes 376 keV by the sum of 198 keV and 178 keV itself. Detailed characteristics related to γ-ray transitions are shown in Table I. γ-ray energies were estimated by fitting a Gaussian function

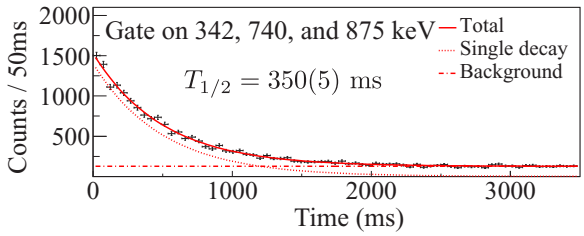

FIG. 2. A decay curve induced by the 342, 740, and 875 keV transitions in ^{140}I. The red solid line is the result of the fit using an exponential decay curve and a constant background. The measured half-life is shown and the number in parentheses is an error in the last digit.

and Compton background. Uncertainties were determined by the standard errors of the mean and fit errors in principle and energies without them have smaller uncertainties than the order of the last digit. The 44-keV energy could not be estimated by the above method due to the extremely low intensity. For this energy, the uncertainty was determined by the range which was mostly affected by the bin size of the histogram. The relative γ-ray intensity, I_γ, was deduced by the measured area of Gaussian function for each peak. Measured areas were calibrated by the efficiency of detecting systems, and energies below 400 keV were corrected by the internal conversion effect. To determine the internal conversion coefficients, transitions depopulating 1^+ states were all assigned as $E1$ transitions while other transitions were assumed to be $M1$ transitions. These relative γ-ray intensities were normalized to the intensity of the 51-keV transition, which was the most intense one. More details about γ-γ coincidence energies including those in Fig. 3 are also shown in Table I.

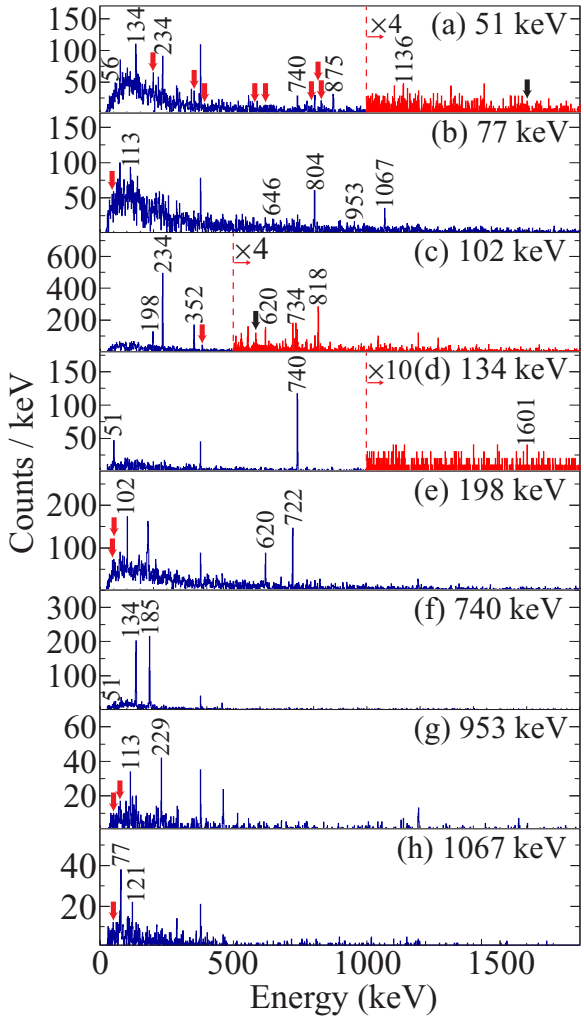

FIG. 3. γ-γ coincidence spectra for 51, 77, 102, 134, 198, 740, 953, and 1067 keV. Coincident peaks are indicated with numbers or arrows. Some regions are enlarged for clarity. The 376-, 458-, and 775-keV peaks are from internal transitions of ^{140}Xe. Unlabeled peaks are random coincident backgrounds.

Figure 4 represents the internal level scheme of ^{140}I which was constructed by γ-γ coincidence methods. The thickness of each transition implies the intensity based on information in Table I. For energies lower than 300 keV, the ratios between filled and empty spaces depict internal electron conversion ratios. According to the feeding properties of the excited levels of ^{140}Xe, the spin-parity of the ground state of ^{140}I was assigned as (2^-). We emphasize that there are two β-decay branches: one is built from the (4^-) state, as already known [16], via the direct β decay of $^{140}\text{I} \rightarrow {}^{140}\text{Xe}$, and the other is built from the (2^-) state which is the case of this work: the $^{140}\text{Te} \rightarrow {}^{140}\text{I} \rightarrow {}^{140}\text{Xe}$ β-decay branch [17].

All spin-parity assignments are based on not only the log ft value arguments—i.e., states with log ft values of 5.5–6.5 are assigned as the first forbidden transitions [18–21]—but also the shell model calculations. Levels at 926, 1188, and 1787 keV are (1^+) states based on the log ft values of 4.89(6), 5.32(6), and 5.96(10), respectively, and the results from the shell model calculations as shown in Fig. 5(a). A strong feeding state at 342 keV, assigned as (0^-) or (1^-), is most likely due to a fast-forbidden transition, indicating the log ft values of 5.2 to 5.5 [22]. The 5.4-keV level is likely to be a (1^-) state based on the shell model calculations. Levels with a direct transition to the ground state are assigned as (1^-) or (2^-) by assuming that all transitions are $M1$.

IV. DISCUSSION

A. Shell model calculation

In order to assign proton-neutron configurations to the states presented in Fig. 4, we performed large-scale shell model calculations in the full $50 < Z < 82$ and $82 < N < 126$ model spaces. The potential used in these calculations was the charge dependent Bonn potential, based on the realistic CWG Hamiltonian [22,23] in the $Z50N82$ model space. The calculations were carried out using the shell model code KSHELL [24]. In Fig. 5, both theoretical and experimental results are shown with the comparison between ^{136}I and ^{140}I in terms of (a) energy levels, (b) configurations, and (c) G-T strength. It should be emphasized that there are no data for the case of ^{138}I associated with β decay.

The shell model calculations for the 1^+ states show a clear contrast between ^{136}I and ^{140}I. In the case of ^{140}I, there is a large difference in not only the position of the 1^+ state by 0.5 MeV but also the G-T strength by a few tens

TABLE I. A summary of E_γ, multipole, relative γ-ray intensities, I_γ, placements, and coincidence γ rays in the observed γ-ray transitions in ^{140}I. The number in the parentheses is an error in the last digit.

E_γ (keV)	Multipole[a]	I_γ(%)[b]	$E_{\text{level},i}$ (keV)	$E_{\text{level},f}$ (keV)	Coincidences (keV)
44.0(<1.0)	$M1$	64.2(7.4)	44.0	0	77, 113, 646, 804, 953, 1067, 1552
51.4	$M1$	100(6)	51.4	0	56, 198, 134, 234, 352, 383, 583, 620, 734, 740 790, 818, 830, 875, 1136, 1601
56.0(1)	$M1$	33.6(5.0)	107.4	51.4	51, 234, 352, 383, 583, 620, 734, 818
77.7(1)	$M1$	47.9(5.5)	121.3	44.0	44, 113, 646, 804, 953, 1067, 1552
102.0	$M1$	52.4(3.4)	107.4	5.5	198, 234, 352, 383, 583, 620, 734, 818
113.8(2)	$M1$	8.42(1.23)	235.1	121.3	44, 77, 646, 953, 1552
120.9(1)	$M1$	6.17(71)	121.3	0	113, 646, 804, 953, 1067, 1552
134.2	$M1$	13.6(1.1)	185.6	51.4	51, 740, 1601
142.4	$M1$	15.8(1.2)	142.4	0	497, 783, 1046, 1644
185.6	$M1$	13.9(1.1)	185.6	0	740, 1601
198.1	$E1$	21.7(1.6)	925.5	727.7	51, 56, 102, 620, 722
229.4	$M1$	6.47(63)	235.1	5.5	646, 953, 1552
234.5	$M1$	24.9(1.6)	342.0	107.4	51, 56, 102, 583
342.1	$M1$	26.8(1.6)	342.0	0	583
351.9	$M1$	12.3(9)	459.4	107.4	51, 56, 102
382.6	$M1$	3.09(19)	490.0	107.4	51, 56, 102, 435
435.2(1)	$E1$	2.34(51)	925.5	490.0	51, 56, 102, 383
497.0(1)	$M1$	2.59(47)	639.4	142.4	142
583.3(2)	$E1$	2.15(53)	925.5	342.0	51, 56, 102, 234, 342
620.3(1)	$M1$	7.58(87)	727.7	107.4	51, 56, 102, 198
646.5(2)	$M1$	2.47(51)	881.4	235.1	44, 77, 113, 229
722.3	$M1$	10.7(7)	727.7	5.5	198
734.7(1)	$M1$	3.47(1.68)	842.0	107.4	51, 56, 102
739.8	$E1$	29.1(1.7)	925.5	185.6	51, 134, 185
783.3	$E1$	6.31(56)	925.5	142.4	142
790.6(1)	$M1$	5.16(51)	842.0	51.4	51
804.5(2)	$E1$	14.9(1.7)	925.5	121.3	44, 77, 121
817.8	$E1$	7.54(69)	925.5	107.4	51, 56, 102
830.0	$M1$	6.90(61)	881.4	51.4	51
875.0	$E1$	25.5(1.6)	925.5	51.4	51
925.1(2)	$E1$	4.55(94)	925.5	0	
952.9	$E1$	8.27(73)	1188.2	235.1	44, 77, 113, 229
1045.7(3)	$E1$	0.903(449)	1188.2	142.4	142
1067.1	$E1$	6.21(58)	1188.2	121.3	44, 77, 121
1136.4	$E1$	14.4(9)	1188.2	51.4	51
1188.5(3)	$E1$	2.41(72)	1188.2	0	
1551.6(4)	$E1$	0.639(405)	1786.9	235.1	44, 77, 113, 229
1601.1(2)	$E1$	2.11(39)	1786.9	185.6	51, 134, 185
1644.5(2)	$E1$	1.09(43)	1786.9	142.4	142
1787.2(2)	$E1$	0.911(291)	1786.9	0	

[a]γ-ray transitions from 1^+ states are all assigned as $E1$ transitions. Other transitions are assumed to be $M1$ transitions.
[b]The relative γ-ray intensity, I_γ, is normalized to the intensity of the 51.4-keV transition. Intensities for transitions below 400 keV are corrected by internal conversion coefficients.

of magnitude. For ^{136}I, the calculations show a reasonable agreement with the experimental data in terms of excited levels, including the three 1^+ states at 2.5–3.3 MeV. Although the expected G-T strengths are not fairly reproducible, it is noteworthy, as shown in Fig. 5(c), that the calculated total strength, indicating a G-T strength of about 0.22, is almost identical to the sum of the experimental values of the three 1^+ states [25]. Consequently, the experimental data suggest that the occupancy of the $\nu h_{9/2}$ orbital should be comparable to that of 1^+_1 in calculations, giving rise to appreciable G-T strengths for the three 1^+ states. Turning our attention to the properties of the occupancies as shown in Fig. 5(b) we find, first, that the 1^+ states are formed due to a large contribution of protons in the $h_{11/2}$ orbital and neutrons in the $h_{9/2}$ orbital. It is apparent that a dominant occupancy in the $\nu h_{9/2}$ orbital gives rise to a strong G-T strength by the coupling to the proton-dominant $h_{11/2}$ orbital. Second, there is a significant difference in the proton $g_{7/2}$ and $d_{5/2}$ orbital occupancies between ^{136}I and ^{140}I, yielding different proton-neutron mixed configurations when increasing the number of neutrons. It

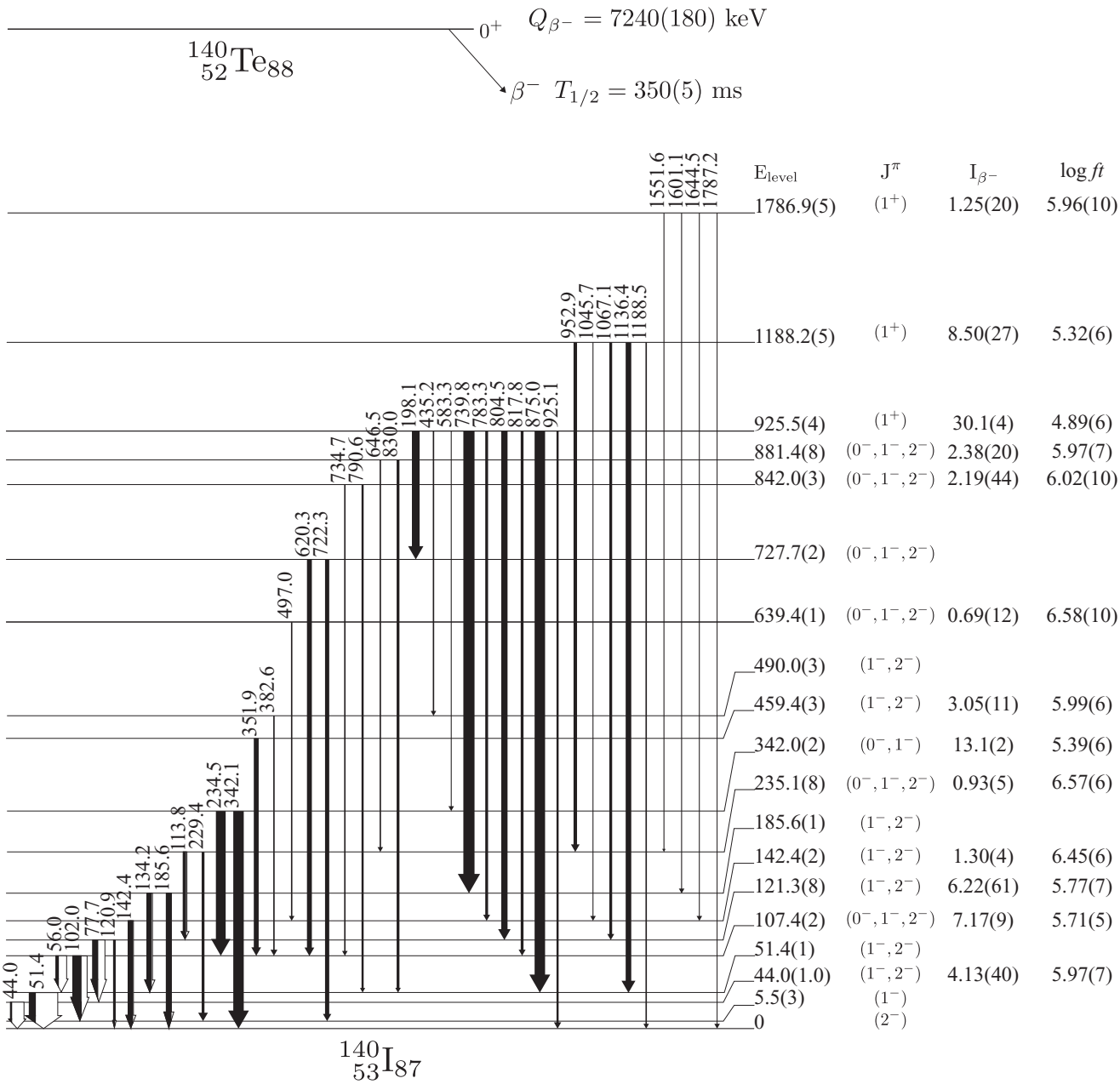

FIG. 4. A partial level scheme of ^{140}I as deduced from the β decay of ^{140}Te. The intensities of the low-lying transitions were corrected for the electron conversion by assuming an $M1$ character. Energies are given in keV and I_{β^-} values are given in %. The number in the parentheses is an error in the last digit.

should be noticed that their evolution is described in terms of the neutron skin [10]. The large difference of ^{140}I between theory and experiment indicates that the G-T strength is very sensitive to the nuclear structure associated with proton-neutron configurations at low-lying energies. Such a large deviation of the G-T strengths provides an insight that the used interaction should be improved for reliable predictability. For the case of ^{136}I, in contrast, such a large deviation does not appear, showing better agreement between theory and experimental data. As already pointed out, the theoretical calculation represents the G-T strength becomes enhanced in ^{140}I; however, in the experimental result, the G-T strength becomes suppressed in ^{140}I. These aspects indicate that the nuclear structure changes as the neutron number increases beyond the $N = 82$ shell closure. The low-lying position of the 1^+ state may be a consequence of the onset of deformation at $N = 87$, in contrast to the spherical shape at $N = 83$ [27].

B. Nilsson model calculation

In order to obtain a physically consistent picture of the aspects involved in the decay of ^{140}Te to ^{140}I, the deformed shell model calculation based on the Nilsson orbitals [29] was performed. The Nilsson-BCS model including pairing correlation calculations defines a deformed quasiparticle basis with an asymptotic quantum number, $[N,n_z,\Lambda]\Omega(=\Lambda+\Sigma)$.

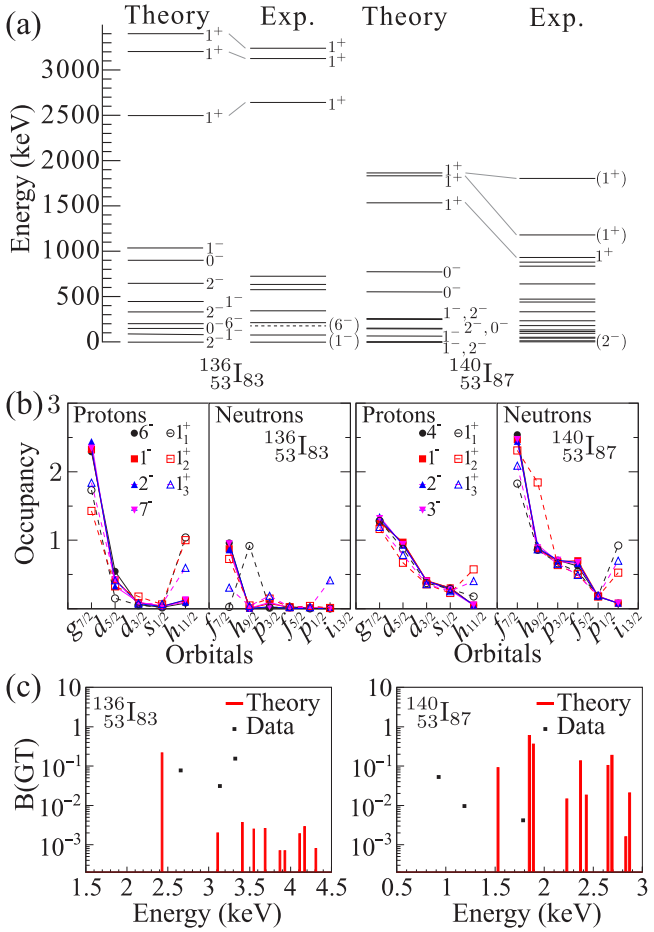

FIG. 5. (a) The calculated level energies based on a large-scale shell model with the CWG nucleon-nucleon interaction Hamiltonian for ^{136}I (left) and ^{140}I (right). Experimental results for ^{136}I are from [16,25,26] and those for ^{140}I are from the present work. (b) Proton and neutron number occupancy distributions in the orbitals associated with the formation of the first few negative parity states of interest and the first three 1^+ states for ^{136}I (left) and for ^{140}I (right). (c) Theoretical (red histogram) and experimental (squares) G-T strength distributions.

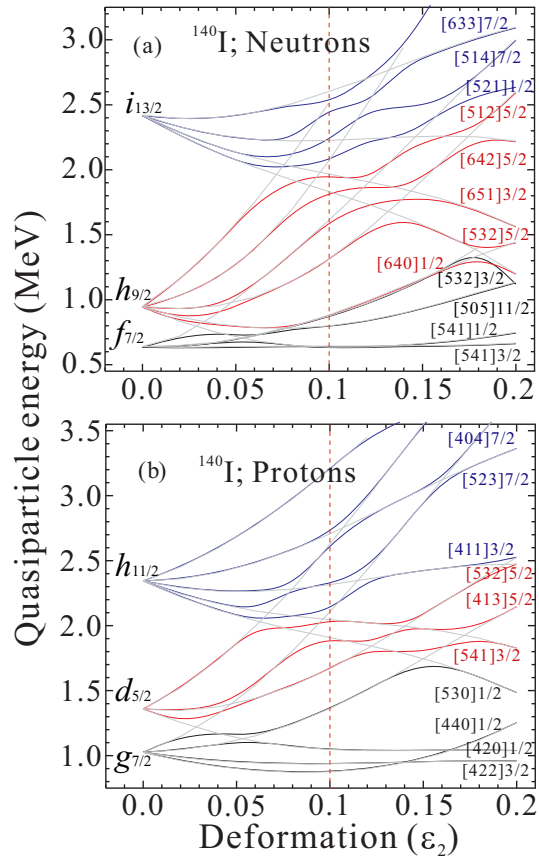

FIG. 6. Calculated quasiparticle energy diagrams for ^{140}I, based on the deformed Nilsson model as a function of quadrupole deformation parameter, ϵ_2. The used pairing parameters are $\Delta_p = 0.873$ MeV for quasiprotons and $\Delta_n = 0.628$ MeV for quasineutrons deduced from the atomic mass evaluation [28]. The Nilsson orbitals are labeled by the asymptotic quantum number $[N,n_z,\Lambda]\Omega$. The grey lines represent diabatic trajectories originated from a spherical orbital. Red dot lines at $\epsilon_2 = 0.1$ are regions of interest in this work.

The quasiparticle energies were obtained by summing their respective energies given by $E_x = \sqrt{(E-\lambda)^2 + \Delta_{p,n}^2}$, where E is the single proton or neutron energy from the Hartree-Fock calculations, λ is the Fermi level, and $\Delta_{p,n}$ are the proton or neutron pairing strength parameters. The pairing parameters used in this work were $\Delta_p = 0.873$ MeV for protons and $\Delta_n = 0.628$ MeV for neutrons, which are deduced from the recent atomic mass evaluation [28]. Figure 6 shows the result for quasiparticle excitation energies, in the space of three major shells $N = 3,4,5$ for protons and $N = 4,5,6$ for neutrons as a function of the deformation quadrupole parameter, ϵ_2. It should be noted that the configuration is plotted based on the adiabatic trajectory. To understand the original spherical orbital trajectory, the diabatic lines are also included.

At a small deformation of $\epsilon_2 \sim 0.1$, the observed G-T transitions are possible from the proton-neutron interactions between the [541]3/2, [541]1/2, [532]5/2, [532]3/2 orbitals for neutrons and the [530]1/2, [541]3/2, [532]5/2 for protons. Thus, the most favorable β-decay path to a 1^+ state involves the ν[541]1/2 to π[541]3/2 transition which is related to an allowed G-T transition as $\Delta n_z = 0$, $\Delta\Lambda = 0$, and $\Delta\Omega = 1$. It is important to point out that both orbitals retain significantly the spherical $\nu h_{9/2}$ and $\pi h_{11/2}$ character. This $\pi h_{11/2}$[541]3/2$\nu h_{9/2}$[541]1/2 configuration, predicted near 1100 keV, is most likely responsible for the formation of the 1^+ state observed at 926 keV, leading to the G-T strength with $\log ft = 4.89(6)$. The weakly populated G-T transition at 1188 keV may be due to the $\pi h_{11/2}$[532]5/2$\nu h_{9/2}$[532]3/2 configuration. We note that similar transitions to the $[\pi h_{11/2}\nu h_{9/2}]1^+$ configuration have been commonly observed in odd-odd La nuclei with $Z = 57$ [30–33]. It has been reported that a group of allowed β decays in the rare-earth region have their $\log ft$ values of 4.5 to 5.0 [34]. For example, the $\log ft$ values for the known G-T transitions connecting the nuclei of Ho ($Z = 67$) isotopic sequence with $N > 82$ nuclei indicate a $\log ft$ of around 4.7. The related transitions, for Ho isotopes, were explained in terms of the transformation due to a $\pi h_{11/2}$ to

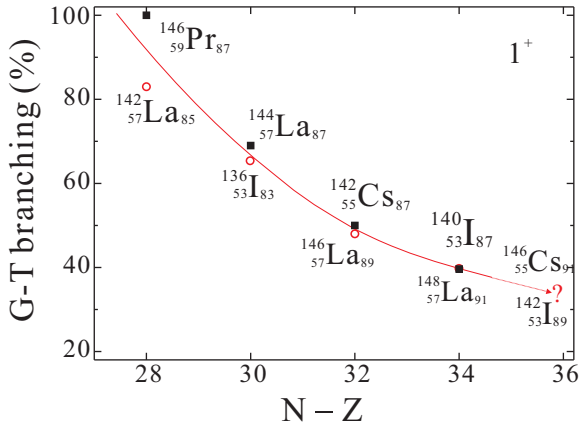

FIG. 7. Systematic features of the β-decay branching ratios, indicating percentage of the G-T distribution, to the low-lying 1^+ states built on the $\pi h_{11/2}\nu h_{9/2}$ configuration in odd-odd nuclei as a function of the neutron-proton difference, $N - Z$; along the isotones (filled squares) with $N = 87$ and isotopes La and I (empty circles). The grey (red online) line represents an assumed trend to guide the eye. For future investigation, we add nuclides with $N - Z = 36$: ^{142}I and ^{146}Cs.

$\nu h_{9/2}$ in spherical nuclei with $82 \leqslant N \leqslant 86$, the [532] orbital pair in the $N = 87$ transitional nuclei, and the [523] orbital pair in the well deformed nuclei with $N > 88$.

C. Systematic approach

Although the Nilsson model calculations provide good agreements with the suppressed energies, they do not allow the B(GT) value to be extracted from the results. Thus, to understand the relatively weak G-T strength of ^{140}I compared to ^{136}I, we have made systematic estimates with respect to the β-branching ratio to 1^+ states, as a percentage of β decays induced by the G-T transition, in odd-odd nuclei along $N = 87$ isotones. For instance, the data point for ^{140}I has 39.9% of the β-branching ratio of three 1^+ states 926, 1188, and 1787 keV. In addition, we include other neighboring nuclei in order to verify the certainty of the related systematics. As shown in Fig. 7, the percentage of G-T distributions to the lower-lying 1^+ states varies systematically with respect to the neutron and proton number difference, $N - Z$. We observe a significant reduction when this isospin asymmetric parameter is increased, such that, at $N - Z = 28$ the G-T branching is almost 100% while at $N - Z = 34$ it is down to near 40%. A conclusion that can be drawn from the present systematic study is that the G-T branching is expected to be around 30% for the nuclei with $N - Z = 36$: ^{142}I and ^{146}Cs. This quenching aspect with the dependence of $N - Z$ (the more neutron rich, the more the reduction) supports the suppression of the G-T strengths in ^{140}I. Consequently, based on the systematics of the G-T branching and the agreement with the Nilsson model, as the isospin, $T_z = (N - Z)/2$, increases in this region, we conclude that the structure of these nuclei becomes more neutron-dominant and deformed. For describing more specifically this effect, the associated quenching factors with spin-flip interactions depending on the isospin value $T_z = (N - Z)/2$ are needed. Therefore, this new result strongly motivates future measurements of the neutron-rich nuclides with $N - Z = 36$ and beyond.

V. CONCLUSION

In conclusion, we have provided, for the first time, the excited states of the neutron-rich nucleus ^{140}I through the β decay of ^{140}Te with the half-life of 350(5) ms. The level at 926 keV was suggested to be a (1^+) state on the basis of the log ft value, 4.89(6). The structure of this (1^+) level is interpreted as being associated with the G-T transition between a neutron in the $h_{9/2}$ orbital and a proton in the $h_{11/2}$ orbital. It is evident that shell model calculations do not describe the observed suppression of the G-T strengths and the energies of the newly observed 1^+ states in ^{140}I, in contrast to the reasonable agreement with the experimental result in ^{136}I. Such a suppression of the energies can be described in terms of the deformed shell model calculation based on the Nilsson model, especially with the $\pi h_{11/2}[541]3/2\nu h_{9/2}[541]1/2$ configuration. The present aspect of the G-T response at low-lying energies, with respect to the isospin value of $T_z = (N - Z)/2$, supports the suppression of the G-T strengths. In turn, this result implies that the proton-neutron interaction between the spin-orbital partners is crucially constrained by an excess distribution of neutrons over protons.

ACKNOWLEDGMENTS

This work was carried out at the RIBF operated by RIKEN Nishina Center, RIKEN, and CNS, University of Tokyo. We acknowledge the EUROBALL Owners Committee for the loan of germanium detectors and the PreSpec Collaboration for the readout electronics of the cluster detectors. Part of the WAS3ABi was supported by the Rare Isotope Science Project, which is funded by the Ministry of Science, ICT and Future Planning (MSIP) and National Research Foundation (NRF) of Korea. This research was partly supported by JSPS KAKENHI Grant No. 25247045 and the National Research Foundation grants funded by the Korean government (Grants No. NRF-2009-0093817, No. NRF-2013R1A1A2063017, No. NRF-2016K1A3A7A09005575, and No. NRF-2016K1A3A7A09005578). The FR-JP LIA support is also acknowledged. The shell model calculation research was supported by The National Natural Science Foundation of China under Grant No. 11305272, the Special Program for Applied Research on Super Computation of the NSFC Guangdong Joint Fund (the second phase).

[1] C. E. Rolfs and W. S. Rodney, *Cauldrons in the Cosmos* (The University of Chicago Press, Chicago, 1988).

[2] D. Arnett, *Supernovae and Nucleosynthesis* (Princeton University Press, Princeton, 1996).

[3] H. Schatz, Phys. Today **61**(11), 40 (2008).

[4] J. J. Cowan, F.-K. Thielemann, and J. W. Truran, Phys. Rep. **208**, 267 (1991).

[5] M. Mumpower, R. Suman, D. L. Fang, M. Beard, and A. Aprahama, J. Phys. G: Nucl. Part. Phys. **42**, 034027 (2015).

[6] P. Urkedal, X. Z. Zhang, and I. Hamamoto, Phys. Rev. C **64**, 054304 (2001).

[7] B. Rubio and W. Gelletly, in *The Euroschool Lectures on Physics with Exotic Beams, Vol. III*, edited by J. S. Al-Khalili and E. Roeckl, Lecture Notes in Physics Vol. 764 (Springer, Berlin, 2009), p. 99.

[8] D. C. Radford, C. Baktash, J. R. Beene, B. Fuentes, A. Galindo-Uribarri, C. J. Gross, P. A. Hausladen, T. A. Lewis, P. E. Mueller, E. Padilla, D. Shapira, D. W. Stracener, C.-H. Yu, C. J. Barton, M. A. Caprio, L. Coraggio, A. Covello, A. Gargano, D. J. Hartley, and N. V. Zamfir, Phys. Rev. Lett. **88**, 222501 (2002).

[9] P. Lee, C.-B. Moon, C. S. Lee, A. Odahara, R. Lozeva, A. Yagi, S. Nishimura, P. Doornenbal, G. Lorusso, P.-A. Söderström, T. Sumikama, H. Watanabe, T. Isobe, H. Baba, H. Sakurai, F. Browne, R. Daido, Y. Fang, H. Nishibata, Z. Patel, S. Rice, L. Sinclair, J. Wu, Z. Y. Xu, R. Yokoyama, T. Kubo, N. Inabe, H. Suzuki, N. Fukuda, D. Kameda, H. Takeda, D. S. Ahn, D. Murai, F. L. Bello Garrote, J. M. Daugas, F. Didierjean, E. Ideguchi, T. Ishigaki, H. S. Jung, T. Komatsubara, Y. K. Kwon, S. Morimoto, M. Niikura, I. Nishizuka, and K. Tshoo, Phys. Rev. C **92**, 044320 (2015).

[10] R. Lozeva, H. Naïdja, F. Nowacki, J. Dudek, A. Odahara, C.-B. Moon, S. Nishimura, P. Doornenbal, J.-M. Daugas, P.-A. Söderström, T. Sumikama, G. Lorusso, J. Wu, Z. Y. Xu, H. Baba, F. Browne, R. Daido, Y. Fang, T. Isobe, I. Kojouharov, N. Kurz, Z. Patel, S. Rice, H. Sakurai, H. Schaffner, L. Sinclair, H. Watanabe, A. Yagi, R. Yokoyama, T. Kubo, N. Inabe, H. Suzuki, N. Fukuda, D. Kameda, H. Takeda, D. S. Ahn, D. Murai, F. L. Bello Garrote, F. Didierjean, E. Ideguchi, T. Ishigaki, H. S. Jung, T. Komatsubara, Y. K. Kwon, P. Lee, C. S. Lee, S. Morimoto, M. Niikura, H. Nishibata, and I. Nishizuka, Phys. Rev. C **93**, 014316 (2016).

[11] B. Moon, C.-B. Moon, P.-A. Söderström, A. Odahara, R. Lozeva, B. Hong, F. Browne, H. S. Jung, P. Lee, C. S. Lee, A. Yagi, C. Yuan, S. Nishimura, P. Doornenbal, G. Lorusso, T. Sumikama, H. Watanabe, I. Kojouharov, T. Isobe, H. Baba, H. Sakurai, R. Daido, Y. Fang, H. Nishibata, Z. Patel, S. Rice, L. Sinclair, J. Wu, Z. Y. Xu, R. Yokoyama, T. Kubo, N. Inabe, H. Suzuki, N. Fukuda, D. Kameda, H. Takeda, D. S. Ahn, Y. Shimizu, D. Murai, F. L. Bello Garrote, J. M. Daugas, F. Didierjean, E. Ideguchi, T. Ishigaki, S. Morimoto, M. Niikura, I. Nishizuka, T. Komatsubara, Y. K. Kwon, and K. Tshoo, Phys. Rev. C **95**, 044322 (2017).

[12] T. Kubo, D. Kameda, H. Suzuki, N. Fukuda, H. Takeda, Y. Yanagisawa, M. Ohtake, K. Kusaka, K. Yoshida, N. Inabe, T. Ohnishi, A. Yoshida, K. Tanaka, and Y. Mizoi, Prog. Theor. Exp. Phys. **2012**, 03C003 (2012).

[13] N. Fukuda, T. Kubo, T. Ohnishi, N. Inabe, H. Takeda, D. Kameda, and H. Suzuki, Nucl. Instrum. Methods Phys. Res., Sect. B **317**, 323 (2013).

[14] S. Nishimura, Prog. Theor. Exp. Phys. **2012**, 03C006 (2012).

[15] P.-A. Söderström, S. Nishimura, P. Doornenbal, G. Lorusso, T. Sumikama, H. Watanabe, Z. Y. Xu, H. Baba, F. Browne, S. Go, G. Gey, T. Isobe, H.-S. Jung, G. D. Kim, Y.-K. Kim, I. Kojouharov, N. Kurz, Y. K. Kwon, Z. Li, K. Moschner, T. Nakao, H. Nishibata, M. Nishimura, A. Odahara, H. Sakurai, H. Schaffner, T. Shimoda, J. Taprogge, Zs. Vajta, V. Werner, J. Wu, A. Yagi, and K. Yoshinaga, Nucl. Instrum. Methods Phys. Res., Sect. B **317**, 649 (2013).

[16] National Nuclear Data Center, Brookhaven National Laboratory, http://www.nndc.bnl.gov.

[17] A. Yagi, A. Odahara, *et al.* (priviate communication).

[18] B. Singh, J. L. Rodriguez, S. S. M. Wong, and J. K. Tuli, Nucl. Data Sheets **84**, 487 (1998).

[19] H. Abele, M. A. Hoffmann, S. Baeßler, D. Dubbers, F. Glück, U. Müller, V. Nesvizhevsky, J. Reich, and O. Zimmer, Phys. Rev. Lett. **88**, 211801 (2002).

[20] B. Rubio, W. Gelletly, E. Nácher, A. Algora, J. L. Taín, A. Pérez, and L. Caballero, J. Phys. G: Nucl. Part. Phys. **31**, S1477 (2005).

[21] S. Raman and N. B. Gove, Phys. Rev. C **7**, 1995 (1973).

[22] W.-T. Chou and E. K. Warburton, Phys. Rev. C **45**, 1720 (1992).

[23] B. A. Brown, N. J. Stone, J. R. Stone, I. S. Towner, and M. Hjorth-Jensen, Phys. Rev. C **71**, 044317 (2005).

[24] N. Shimizu, arXiv:1310.5431.

[25] R. B. Firestone and V. S. Shirley, *Table of Isotopes* (John Wiely & Sons, New York, 1996).

[26] W. Urban, M. Saha Sarkar, S. Sarkar, T. Rzaca-Urban, J. L. Durell, A. G. Smith, J. A. Genevey, J. A. Pinston, G. S. Simpson, and I. Ahmad, Eur. Phys. J. A **27**, 257 (2006).

[27] W. Urban, T. Rzaca-Urban, A. Korgul, J. L. Durell, M. J. Leddy, M. A. Jones, W. R. Phillips, A. G. Smith, B. J. Varley, I. Ahmad, L. R. Morss, and N. Schulz, Phys. Rev. C **65**, 024307 (2002).

[28] M. Wang, G. Audi, A. H. Wapstra, F. G. Kondev, M. MacCormik, X. Xu, and B. Pfeiffer, Chin. Phys. C **36**, 1603 (2012).

[29] S. G. Nilsson, C. F. Tsang, A. Sobiczewski, Z. Szymanski, S. Wycech, C. Gustafson, I.-L. Lamm, P. Moller, and B. Nilsson, Nucl. Phys. A **131**, 1 (1969).

[30] C. Chung, W. B. Walters, R. Gill, M. Shmid, R. E. Chrien, and D. S. Brenner, Phys. Rev. C **26**, 1198 (1982).

[31] C. Chung, W. B. Walters, D. S. Brenner, A. Aprahamian, R. L. Gill, M. Shmid, R. E. Chrien, L.-J. Yuan, A. Wolf, and Z. Berant, Phys. Rev. C **28**, 2099 (1983).

[32] C. Chung, W. B. Walters, N. K. Aras, F. K. Wohn, D. S. Brenner, Y. Y. Chu, M. Shmid, R. L. Gill, R. E. Chrien, and L.-J. Yuan, Phys. Rev. C **29**, 592 (1984).

[33] C. Chung, W. B. Walters, D. S. Brenner, R. L. Gill, M. Shmid, Y. Y. Chu, R. E. Chrien, L.-J. Yuan, F. K. Wohn, and R. A. Meyer, Phys. Rev. C **31**, 2199 (1985).

[34] A. K. Jain, R. K. Sheline, D. M. Headly, P. C. Sood, D. G. Burke, I. Hrivnacova, J. Kvasil, D. Nosek, and R. W. Hoff, Rev. Mod. Phys. **70**, 843 (1998).